0026-895X/03/6301-243–252$7.00
MOLECULAR PHARMACOLOGY
Copyright © 2003 The American Society for Pharmacology and Experimental Therapeutics
Mol Pharmacol 63:243–252, 2003

Vol. 63, No. 1
1932/1033374
Printed in U.S.A.

Monomeric and Dimeric Byproducts are the Principal Functional Elements of Higher Order $P2X_1$ Concatamers

ANNETTE NICKE,[1] JÜRGEN RETTINGER, and GÜNTHER SCHMALZING

Department of Molecular Pharmacology, Medical School of the Technical University of Aachen, Aachen, Germany

Received June 14, 2002; accepted October 10, 2002

This article is available online at http://molpharm.aspetjournals.org

ABSTRACT

Heteromultimeric assembly of ion channel subunits generates high diversity in ion channel subtypes with distinct pharmacological and functional properties. To determine the subunit stoichiometry and order of ion channels, constructs with several concatenated subunits have been widely used in electrophysiological studies. Here we used primarily biochemical techniques to analyze the synthesis, assembly, and surface expression of $P2X_1$ concatamers. We found that full-length concatamers consisting of two to six contiguous copies of the $P2X_1$ subunit, although readily synthesized in *Xenopus laevis* oocytes, were entirely retained as aggregates in the endoplasmic reticulum. In contrast, minute levels of lower order byproducts, such as monomers and dimers, that were inherently formed with all the concatamers combined to form defined protein complexes equal in mass to the homotrimeric $P2X_1$ receptor assembled from $P2X_1$ monomers. Besides these complexes consisting of three monomers or one monomer plus one concatenated dimer, only small amounts of concatenated $P2X_1$ trimers reached the plasma membrane. Complexes comprising more than three subunits were not observed in the plasma membrane. The byproduct complexes can account fully for the ATP-gated currents arising from expression of concatenated $P2X_1$ subunits. These results strongly corroborate a trimeric architecture for P2X receptors yet indicate that formation of lower order by-products can be a pitfall of the concatamer approach.

P2X receptors constitute a family of ligand-gated ion channels activated by extracellular ATP (for a review, see Mackenzie et al., 1999). The $P2X_1$ polypeptide contains two transmembrane domains linked by a large, glycosylated extracellular loop (Newbolt et al., 1998; Torres et al., 1998). Like other ligand-gated ion channels, P2X receptors are multimers. Based on the apparent similarity of membrane topology with inwardly rectifying K^+ channels, K_{ir}, and also with the degenerin/epithelial Na^+-channel superfamily, a tetrameric structure seemed to be most plausible. However, results obtained by chemical cross-linking and blue native polyacrylamide gel electrophoresis (BN-PAGE) analysis of receptors assembled from $P2X_1$ or $P2X_3$ polypeptides in *Xenopus laevis* oocytes indicate that trimers represent the essential element of P2X receptors (Nicke et al., 1998). These findings suggest that the P2X receptor provides a fundamentally new structural motif distinct from the established pentameric or tetrameric structures of the other ion channel families.

Methods commonly used to determine the subunit stoichiometry of membrane protein complexes include cross-linking analysis or coprecipitation experiments. However, artifactual aggregation of intracellular proteins resulting from overexpression in heterologous cell systems may severely bias conclusions based on biochemical approaches. In the present study, we used the concatamer approach to confirm the trimeric structure of the P2X receptor and to investigate whether it would be an appropriate method to examine the subunit organization of the P2X receptor. The concatamer strategy has first been applied to voltage-gated K^+ channels, K_v (Isacoff et al., 1990). Linking channel subunits has also been successfully exploited for constraining the stoichiometry of K_v and K_{ir} to identify their quaternary structure (Liman et al., 1992; Yang et al., 1995; Silverman et al., 1996), the gating mechanism (Hurst et al., 1992; Tytgat et al., 1993), positional effects of particular subunits around the pore (Pessia et al., 1996), activation and inactivation mechanisms (Lee et al., 1996), assembly pathways (Tu and Deutsch, 1999), the roles of single amino acid residues for channel function (Hurst et al., 1995; Kirsch et al., 1995), and the nature of subunit-subunit (Lee et al., 1994) and ligand-subunit interactions (Heginbotham and Mackinnon, 1992; Kavanaugh et al., 1992). These predominantly electrophysiological studies indicate that a defined assembly of K^+ channel subunits can be constrained by concatenation. Other mem-

The work was supported by grants SCHM536/2, NI592/2-1, and GRK 137 from the Deutsche Forschungsgemeinschaft.

[1] Present address: Centre for Drug Design and Development, Institute for Molecular Bioscience, University of Queensland, Brisbane, 4072 QLD, Australia.

ABBREVIATIONS: BN-PAGE; blue native polyacrylamide gel electrophoresis; ORi, oocytes Ringer solution; sulfo-SHPP, sulfosuccinimidyl-3-(4-hydroxyphenyl)proprionate; PNGase F, peptide *N*-glycosidase F; DTT, dithiothreitol; ER, endoplasmic reticulum; Endo H, endoglycosidase H.

brane proteins that have been studied by the concatamer approach include close relatives of K^+ channels, such as the cyclic nucleotide-gated channels (Liu et al., 1996; Varnum and Zagotta, 1996; Shapiro and Zagotta, 1998), and hyperpolarization-activated cyclic nucleotide-gated cation channels (Ulens and Tytgat, 2001), but also the ligand-gated $GABA_A$ receptor (Im et al., 1995; Baumann et al., 2001), the mechanosensitive channel of *Escherichia coli* (Blount et al., 1996), the epithelial Na^+ channel (Firsov et al., 1998), aquaporin (Mathai and Agre, 1999), as well as transmembrane transporters (Emerick and Fambrough, 1993; Sahin-Tóth et al., 1994; Köhler et al., 2000). A majority of these studies yielded convincing results, indicating that the concatamers are generated in full length and that the stoichiometry of the resulting ion channels can be constrained by the order in which different ion channel subunits are linked together. However, other reports suggest that concatamers can disrupt the normal association of subunits or that subunits from different concatamers might combine to form one ion channel, whereas adjacent subunits are excluded from the channel (Liman et al., 1992; McCormack et al., 1992; Hurst et al., 1995).

So far, all studies on concatamers depend on the interpretation of electrophysiological properties of the respective constructs. Here we present the first direct investigation of the assembly and surface appearance of oocyte-expressed concatamers. Biochemical analysis of the plasma membrane-bound receptor protein, but not of the total receptor protein, clearly demonstrates that monomeric and dimeric byproducts are generated upon expression of concatenated $P2X_1$ constructs, which appear as a complex equivalent to the plasma membrane-bound homotrimeric $P2X_1$ receptor assembled from wild-type monomers. These $P2X_1$ trimer-equivalent complexes can fully account for the ATP-dependent currents in these oocytes, thus indicating that formation of lower order byproducts can be a pitfall of the concatamer approach.

Materials and Methods

cDNA Constructs. The cDNA construct encoding the N-terminally hexahistidyl-tagged rat $P2X_1$ polypeptide in the vector pNKS2 has been described previously (Nicke et al., 1998). To generate cDNAs encoding $G(Q)_5VMA(H)_6$-linked $P2X_1$ multimers from the dimer up to the hexamer, $(His\text{-}P2X_1)_{2-6}$ (Fig. 1), a double-stranded oligonucleotide (GGGCAGCAGCAGCAGGTCATGAGC and GCTCATGACCTGCTGCTGCTGCTGCCC) encoding five glutamine residues followed by a *Bsp*HI site (underlined) was ligated into the mung bean nuclease-treated C-terminal *Bsu*36I cleavage site of $His\text{-}P2X_1$. This modified $His\text{-}P2X_1\text{-}G(Q)_5V$ cDNA was excised with *Hin*dIII and *Bsp*HI and ligated in frame between the unique *Hin*dIII and *Nco*I cleavage sites of the parent $His\text{-}P2X_1$ plasmid. Because *Nco*I and *Bsp*HI generate compatible cohesive ends that are not recleavable after ligation, this cloning strategy can be repeated many times to engineer concatenated cDNAs encoding $G(Q)_5VMA(H)_6$-linked $P2X_1$ multimers of the desired order. Site-directed mutagenesis was performed using the QuikChange kit (Stratagene, Heidelberg, Germany). Junction sequences and mutations were confirmed by sequencing.

Expression in *X. laevis* Oocytes. Capped cRNAs were synthesized from linearized plasmid cDNAs. Oocytes were prepared as described previously (Nicke et al., 1998), injected with 50-nl aliquots of cRNA (0.5 $\mu g/\mu l$), and kept at 19°C in ORi (oocyte Ringer solution, 90 mM NaCl, 1 mM KCl, 1 mM $CaCl_2$, 1 mM $MgCl_2$, and 10 mM HEPES, pH 7.4) supplemented with 50 mg/l of gentamicin.

Two-Electrode Voltage Clamp Recordings. Current responses to ATP were measured by two-electrode voltage clamp recordings on cRNA-injected oocytes (Rettinger et al., 2000). For determination of current magnitudes, the response to the first application of 30 μM ATP was used.

Radiolabeling of Oocytes. cRNA-injected oocytes and noninjected control oocytes were metabolically labeled by overnight incubation with L-[^{35}S]methionine (>40 TBq/mmol; Amersham Biosciences Europe, Freiburg, Germany) at ~100 MBq/ml in ORi (0.2 MBq/oocyte) at 19°C and cultured in parallel with the nonlabeled oocytes used for surface radioiodination. For selective labeling of plasma membrane bound proteins, cRNA-injected oocytes were kept for 3 days at 19°C and then labeled with freshly radioiodinated ($Na^{125}I$; Amersham Biosciences) sulfosuccinimidyl-3-(4-hydroxyphenyl)proprionate (sulfo-SHPP; Pierce Biotechnology). After 60 min of incubation on ice oocytes were washed in Ca^{2+}-free ORi containing 1 mM lysine to quench unbound ^{125}I-sulfo-SHPP.

Ni^{2+} NTA Affinity Chromatography, Blue Native PAGE, and SDS-PAGE. Proteins were purified from digitonin or dodecyl maltoside extracts of oocytes and resolved by blue native PAGE (Schägger et al., 1994) as described previously (Nicke et al., 1998). For SDS-PAGE, proteins were supplemented with SDS sample

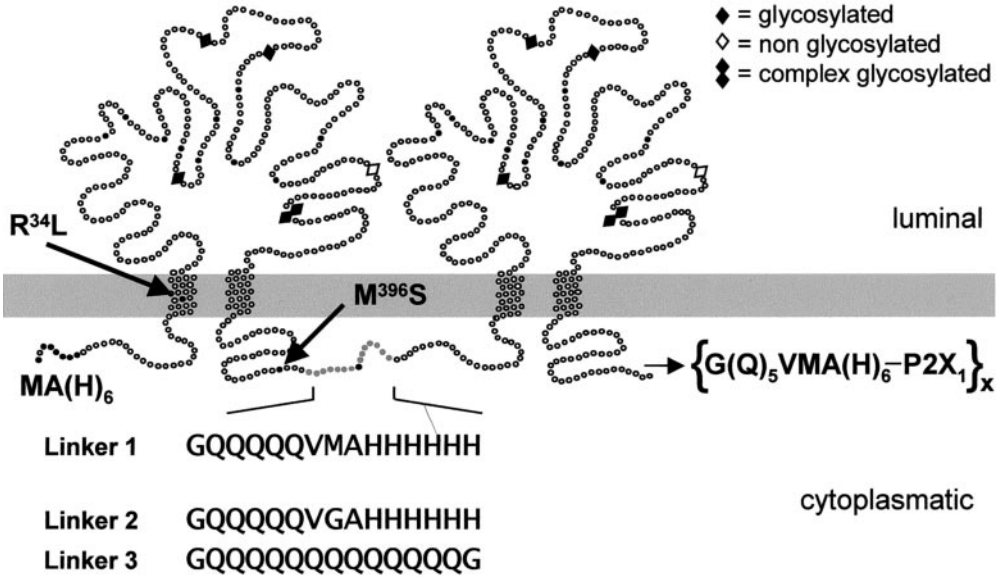

Fig. 1. Schematic diagram of $P2X_1$ concatamers. $His\text{-}P2X_1$ monomers were joined tail to-head with five Q residues, yielding a $G(Q)_5VMA(H)_6$ linking sequence (linker 1). Positions of the four *N*-X-S/T *N*-glycosylation sequons that carry *N*-glycans (Rettinger et al., 2000) are marked by diamonds.

buffer containing 20 mM dithiotreitol (DTT), incubated for 10 min at 37°C, and then electrophoresed in parallel with ^{14}C-labeled molecular mass markers (Rainbow; Amersham Biosciences) on SDS polyacrylamide gels. Where indicated, samples were treated for 1 to 2 h with either endoglycosidase H (Endo H) or PNGase F (New England Biolabs, Frankfurt, Germany) in the presence of reducing SDS sample buffer and 1% (w/v) octylglucoside.

Results

Concatamers of Two to Six Linked $P2X_1$ Monomers All Give Rise to ATP-Gated Cation Currents. We generated a series of concatenated cDNA constructs, $(His\text{-}P2X_1)_{2–6}$, consisting of two to six copies of the His-$P2X_1$ subunit in a single open reading frame by linking together the last C terminal codon of one subunit to the first N terminal codon of the second subunit with a heptapeptide sequence, $G(Q)_5V$ (Fig. 1, linker 1). The resulting cDNAs encode polypeptides of 821, 1235, 1649, 2063, and 2477 amino acid residues. Complementary RNAs were injected into *X. laevis* oocytes, which were subjected to electrophysiological analysis by the two-electrode, voltage-clamp technique 3 days later (Fig. 2). Our hypothesis was that a dimer should give small ATP-gated currents if the functional channel requires three subunits, whereas expression of the trimer should result in considerably larger currents. Contrary to expectations, however, we recorded larger currents in oocytes expressing the concatenated $P2X_1$ dimer (Fig. 2B). This may signify that the functional $P2X_1$ receptor is made up of an even number of subunits, potentially four or six. We therefore analyzed tetrameric, pentameric, and hexameric constructs. However, a tetrameric or hexameric subunit organization was also not supported by the data, because the current magnitude decreased further when higher order concatamers were expressed. We can therefore not infer from these data any preferential formation of functional $P2X_1$ receptors from a particular concatamer. Qualitatively, the ATP-inducible currents recorded from oocytes expressing tandem constructs were virtually identical to those in oocytes expressing the wild-type $P2X_1$ monomer alone, as illustrated by the individual current traces in Fig. 2A.

His-$P2X_1$ Concatamers Are Synthesized with the Expected Masses. When metabolically labeled His-$P2X_1$ concatamers were resolved by reducing SDS-PAGE, the isolated dimers and trimers appeared as bands at about 120 and 180 kDa, respectively (Fig. 3), compared with the monomer, which migrates as a 57- to 64-kDa glycoprotein depending on whether it was resolved on a linear (Fig. 4B) or on a gradient gel (Fig. 3). Concatamers larger than the trimer migrated at positions that are entirely consistent with the expected multiples of a 57-kDa $P2X_1$ monomer when run on linear gels (Fig. 4B), yet tended to migrate somewhat faster on gradient gels (Fig. 3). Nevertheless, the regular decrease in mobility of all the polypeptides with the order of the construct leaves no doubt that each of the five concatamers is synthesized with the expected mass of a full-length protein. Besides full-length concatamers, small amounts of monomeric and dimeric byproducts are visible (Fig. 3, lanes 3–8). Intermediate-sized byproducts smaller than the monomer or located between the monomer and the dimer were never observed.

All Potential *N*-Glycosylation Sites of $P2X_1$ Concatamers Are Used. A single $P2X_1$ polypeptide carries four *N*-glycans on the ectodomain, which increase the mass of the polypeptide by ~18%. To assess whether a given concatamer folds through the membrane with the predicted number of transmembrane segments (Fig. 1), the mass shift caused by full deglycosylation with PNGase F was determined (Fig. 3). To allow for precise mass determinations over the entire mass range, a calibration curve was constructed by plotting the $\log_{10}$ of the masses of the protein cores predicted from the amino acid sequence of the various concatamers against their relative mobilities, thus using the $P2X_1$ concatamers as their own mass standards. Based on this calculation, each concatamer contains virtually the same mass fraction of *N*-linked carbohydrates [17.6 ± 1.2% (mean ± S.D.)] as the parent $P2X_1$ polypeptide. This indicates that the number of *N*-glycans increases in proportion with the number of $P2X_1$ copies incorporated in a concatamer, suggesting that each copy carries four *N*-glycans.

Full-Length $P2X_1$ Concatamers Are Retained as Aggregates in the ER. Because we did not find a preferential

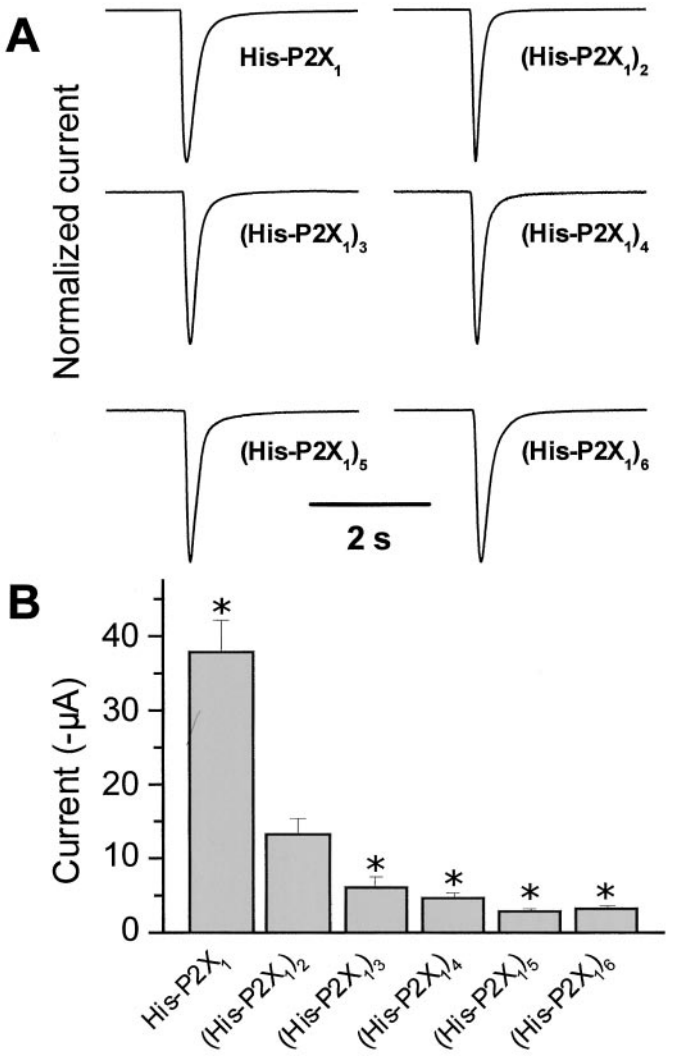

Fig. 2. Comparison of inward current responses generated by expression of $P2X_1$ monomers and concatamers. Currents evoked by 30 μM ATP were recorded at −60 mV from oocytes injected with 25 ng of cRNA for the indicated $P2X_1$ construct 3 days earlier. A, original current traces that have been scaled to the same amplitude for comparison of time courses. B, magnitudes of ATP-induced inward currents decrease with the order of the $P2X_1$ concatamer expressed. Data are given as means ± S.E.M. from five to seven oocytes per column. *, $p < 0.05$, statistically significant difference from His-$P2X_2$ dimer (unpaired Student's *t* test).

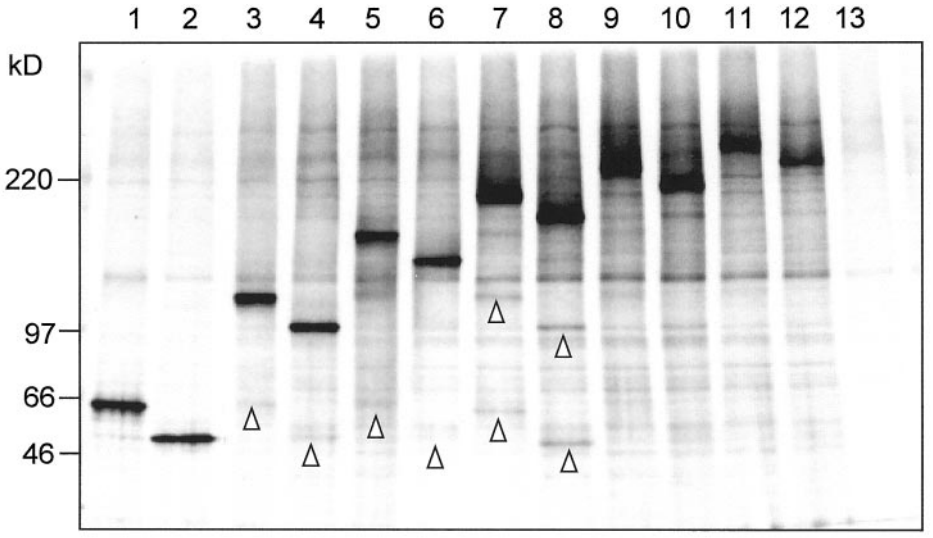

Construct	His-P2X$_1$		(His-P2X$_1$)$_2$		(His-P2X$_1$)$_3$		(His-P2X$_1$)$_4$		(His-P2X$_1$)$_5$		(His-P2X$_1$)$_6$		Contr.
PNGase F	+	–	+	–	+	–	+	–	+	–	+	–	–
ΔkD	8		19		30		40		47		60		–

Fig. 3. Molecular masses and *N*-glycan content of His-P2X$_1$ concatamers. Oocytes were labeled overnight with [^{35}S]methionine and then extracted with digitonin (1%). Proteins were natively purified by Ni^{2+} NTA agarose chromatography, treated with PNGase F as indicated, and resolved by reducing SDS-PAGE (4–10% acrylamide). ΔkD gives the molecular mass shifts induced by deglycosylation. Arrowheads indicate positions of lower order side products.

formation of functional P2X$_1$ receptors with any of the concatamers analyzed, we examined whether concatamers can by themselves homomultimerize into higher order assemblies. This has often been accounted for inconsistencies in the analysis of concatamers. Functional trimeric P2X$_1$ receptors could be generated, for instance, by dimerization of two dimers if one of the two dimers donated only one of its two P2X$_1$ copies to the receptor channel. For oligomer detection, we exploited blue native PAGE analysis, which is able to correctly display the pentameric nature of members of the nicotinic superfamily (Nicke et al., 1998; Griffon et al., 1999). When resolved by blue native PAGE, the P2X$_1$ receptor assembled from P2X$_1$ monomers exhibited a mobility corresponding to that of soluble marker proteins of an apparent molecular mass of approximately 250 kDa (Fig. 4A) as described previously (Nicke et al., 1998). The 250-kDa P2X$_1$ receptor protein consists of three noncovalently linked P2X$_1$ monomers. Reduction with DTT results in a partial dissociation of the 250-kDa protein into two lower-order bands of apparent masses of 170 and 80 kDa, which represent an intermediate dimer and the monomer, respectively (Fig. 4A, lane 6). These masses are larger than those found by SDS-PAGE analysis for the His-P2X$_1$ monomer or the concatenated dimer and trimer, because soluble proteins (used as markers) and membrane proteins can differ in their mobility in the BN-PAGE system (Schägger et al., 1994). Hence, the molecular masses obtained by BN-PAGE analysis must be regarded as relative values rather than absolute values (Nicke et al., 1998).

Surprisingly, when dimeric, trimeric, or tetrameric concatamers were analyzed by blue native PAGE, small amounts of a discrete protein band were observed, which migrated at exactly the same mass (250 kDa) as the homotrimeric P2X$_1$ receptor assembled from expressed monomers (Fig. 4A, lanes 1–4). The bulk of proteins arising from expressed concatamers migrated at a broad range of masses well above the 250-kDa band and, in part, even failed to enter the separating gel. We assume that this large excess of undefined protein complexes represents aggregates of full-length concatamers. Apparently, only P2X$_1$ monomers are able to assemble efficiently into a defined oligomeric state. This view is supported by the observation that the amorphous aggregates could be diminished in favor of a discrete and prominent protein band corresponding to the full-length dimer (Fig. 4A, lane 7), trimer (lane 8), or tetramer (lane 9), when samples were incubated with DTT before blue native PAGE. In addition, DTT treatment disclosed the presence of small amounts of P2X$_1$ monomers, originating apparently from dissociation of the 250-kDa protein, irrespective of whether the oocytes expressed dimers, trimers, or tetrameric P2X$_1$ concatamers. Dissociation of trimeric P2X$_1$ complexes into monomers could also be produced by other denaturing agents such as urea or SDS, indicating that reduction of intramolecular disulfide bonds causes a pertubation of non covalent subunit interactions (Nicke et al., 1998).

Next we examined the carbohydrate status of the concatamers. From the four *N*-glycans of the parent P2X$_1$ polypeptide, one (at N300) exists in the Endo H resistant complex-glycosylated form at the plasma membrane of oocytes (Rettinger et al., 2000). More than 70% of the monomeric His-P2X$_1$ subunits acquired complex-type carbohydrates within a 72-h chase interval (Fig. 4B). Likewise, a large portion of the monomeric byproducts is also obviously in the Endo H-resistant form (Fig. 4B). Hence, if concatamers are efficiently transported out of the ER, they too should acquire Endo H resistance to a significant extent during the chase interval. This, however, is not the case. P2X$_1$ concatamers isolated 3 days after metabolic labeling show little if any complex glycosylation (Fig. 4B), implying that concatamers are either largely unable to leave the ER or that processing by Golgi enzymes of the particular *N*-glycans at N300 and corresponding positions of concatamers is steri-

cally hindered. The latter can be ruled out, because concatenated dimers and trimers that appear at the plasma membrane contain complex-type carbohydrates (Fig. 5B). We conclude from these results that full-length concatamers in *X. laevis* oocytes have a tendency to form large aggregates and hence can hardly exit the ER. A small amount of monomers seems to be inherently formed as a byproduct of larger order $P2X_1$ concatamers. These monomeric byproducts have a strong propensity to assemble to a trimeric $P2X_1$ complex that is visible as a discrete 250-kDa protein band.

The Plasma Membrane Contains Primarily Monomeric and Dimeric Byproducts of Higher Order $P2X_1$ Concatamers. To examine whether full-length concatamers are incorporated into the plasma membrane, the cell surface of intact oocytes was selectively radioiodinated. His-tagged proteins were subsequently purified from digitonin or dodecylmaltoside extracts of these cells. Irrespective of the concatamer expressed, blue native PAGE analysis revealed one discrete 250-kDa protein band that migrated with exactly the same mobility as the noncovalently linked homotrimeric His-$P2X_1$ receptor (Fig. 5A, lanes 1–4). Treatment with DTT resulted in a dissociation of the 250-kDa band into $P2X_1$ dimers and monomers, indicating that the majority of the 250-kDa protein consisted of either three monomers or one

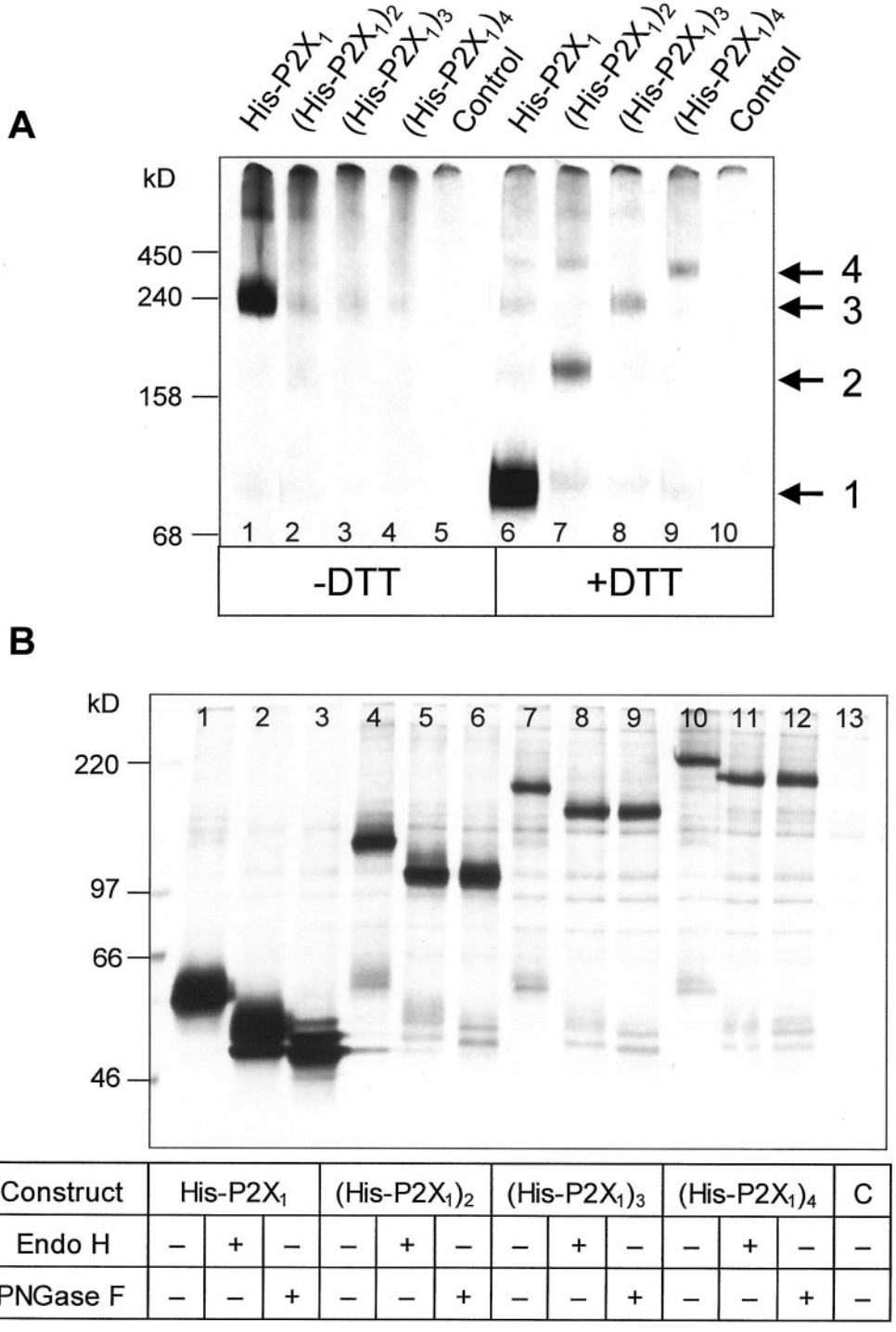

Fig. 4. Oligomeric state and glycosylation state of total (plasma membrane-bound plus intracellular) His-$P2X_1$ concatamers. His-tagged proteins were isolated under nondenaturing conditions from dodecylmaltoside (0.5%) extracts of metabolically labeled oocytes. A, oligomeric state. Protein complexes were resolved by blue native PAGE (5–13% acrylamide) either without further treatment or after incubation for 30 min at 37°C with 0.1 M DTT as indicated. Numbered arrows indicate positions of respective multimers. B, glycosylation state. Aliquots of the samples shown in (A) were treated with Endo H or PNGase F as indicated, and resolved by reducing SDS-PAGE (8% acrylamide). C, noninjected control oocytes.

monomer associated with a concatenated dimer (lanes 6–9). Only minor amounts of concatenated trimers reached the plasma membrane (lane 8). No significant assembly of concatamers resulting in complexes with more than three $P2X_1$ copies occurred. Likewise, no significant surface expression of $(His\text{-}P2X_1)_4$ was observed.

Analysis of the glycosylation status by treatment with Endo H and PNGase F shows that the radioiodinated byproducts originating from the expression of the concatamers behaved like authentic $P2X_1$ polypeptides. From the plasma-membrane-bound $P2X_1$ monomer, three *N*-glycans can be released by Endo H, whereas the fourth *N*-glycan is Endo H-resistant and requires PNGase F treatment to be cleaved off (Fig. 5B, lanes 2–3). Likewise, a similar pattern of bands was obtained for the plasma membrane-bound dimer and trimer, which is consistent with the presence of six and nine core-glycosylated and two and three complex-glycosylated *N*-glycans, respectively (Fig. 5B). Collectively, these results suggest that the plasma membrane-bound concatamers and byproducts exist in a conformation that is not essentially different from that of authentic $His\text{-}P2X_1$ subunits. The absence of an entirely Endo H-sensitive $P2X_1$ polypeptide visi-

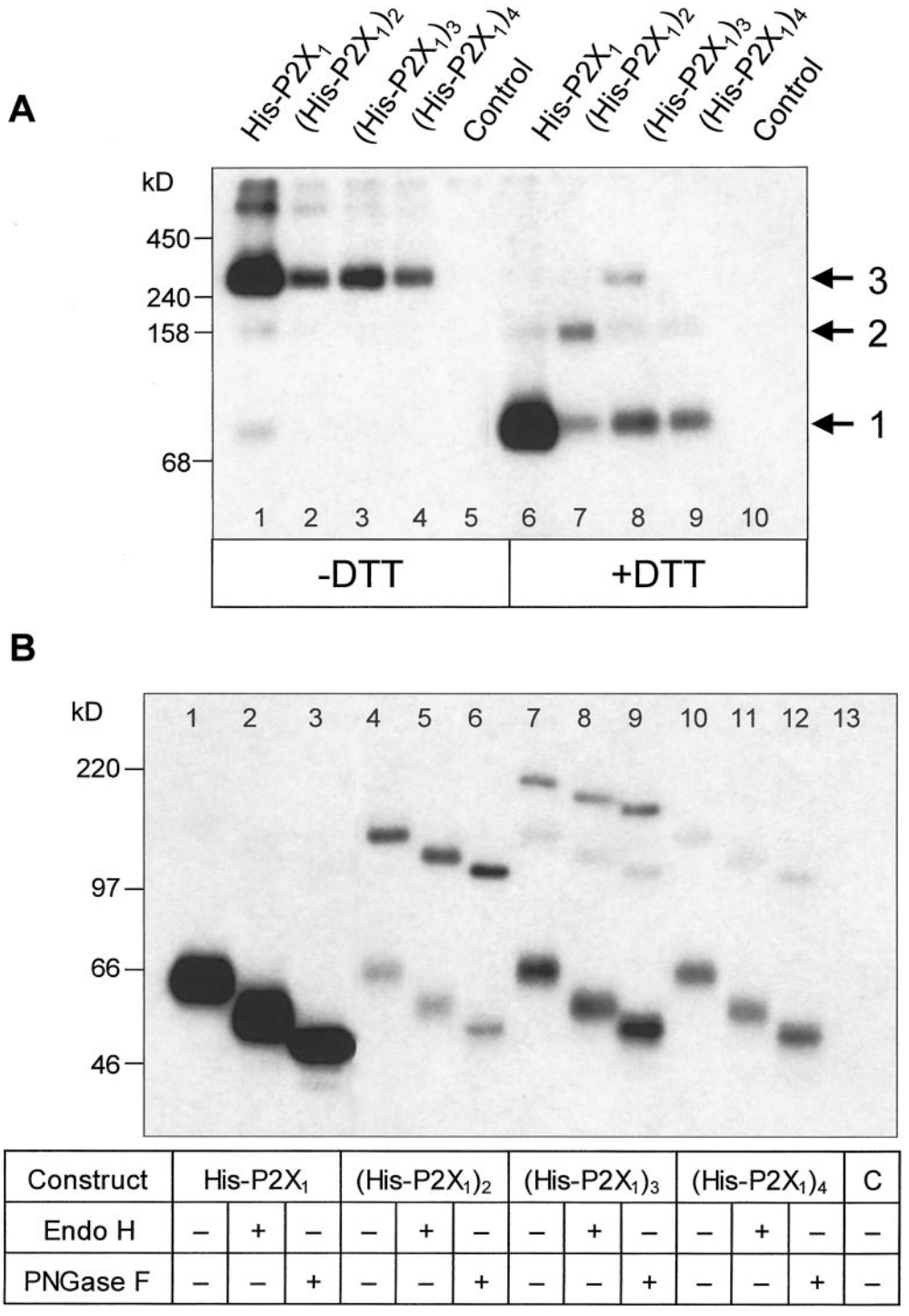

Construct	His-P2X1			(His-P2X1)2			(His-P2X1)3			(His-P2X1)4			C
Endo H	–	+	–	–	+	–	–	+	–	–	+	–	–
PNGase F	–	–	+	–	–	+	–	–	+	–	–	+	–

Fig. 5. Visualization of plasma membrane-bound $P2X_1$ receptor complexes produced from expressed concatamers. His-tagged proteins were isolated under nondenaturing conditions from dodecylmaltoside extracts (0.5%) of oocytes surface-labeled with membrane-impermeant ^{125}I-sulfo-SHPP. A, oligomeric state. Protein complexes were resolved by blue native PAGE (4–13% acrylamide) either without further treatment or after incubation for 30 min at 37°C with 0.1 M DTT as indicated. Numbers beside arrows specify the number of $P2X_1$ copies present in the respective protein either in the form of noncovalently linked monomers or concatamers. Irrespective of the order of the concatamer expressed, the plasma membrane contains only protein complexes equal in mass to the wild-type $P2X_1$ receptor, which is a noncovalently linked homotrimer. Note that the amount of the 250 kDa protein was larger for $(His\text{-}P2X_1)_2$ (lane 2) than for $(His\text{-}P2X_1)_3$ in this particular experiment. In two other experiments, however, more 250-kDa protein was observed after expression of $(His\text{-}P2X_1)_2$ than for higher order concatamers consistent with the current magnitudes shown in Fig. 2B. B, aliquots of the same protein samples were treated with Endo H or PNGase F as indicated and resolved by reducing SDS-PAGE (8% acrylamide).

ble in samples isolated from [^{35}S]methionine-labeled oocytes demonstrates the specificity of the surface radioiodination method.

Monomeric and Dimeric Byproducts Do Not Originate from the Usage of Internal Methionines of Higher Order Concatamers. Internal translation initiation could be a possible source of lower order byproducts. The tandem P2X$_1$ dimer construct contains two AUG codons that, if used as internal initiation codons, would give rise to polypeptides of approximately the size of a P2X$_1$ monomer. One AUG encodes an endogenous methionine, M^{396}, at the very C-terminal end of the N-terminal P2X$_1$ copy, and the second encodes a methionine residue in the linker sequence (Fig. 1, linker 1), designated M^{Linker}. To assess the possible contribution of these internal AUG codons on monomer formation, M^{396} and M^{Linker} were successively changed to serine and glycine, respectively (linker 2). In addition, we engineered a P2X$_1$ dimer with a modified linker consisting almost solely of 13 glutamine residues and lacking in particular the hexahistidyl sequence as well as M^{Linker} (Fig. 1, linker 3). Polyglutamine linkers have been widely used in previous studies for tethering of channel subunits (Isacoff et al., 1990; Hurst et al., 1992; Yang et al., 1995; Pessia et al., 1996; Varnum and Zagotta, 1996; Firsov et al., 1998). The encoded P2X$_1$ dimers were analyzed in respect to plasma membrane appearance of ATP-gated ion channels and protein accessible to surface radioiodination. Replacement of M^{396} or of M^{Linker} together with the hexahistidyl tag did not reduce the magnitude of ATP-gated currents in comparison with the parent P2X$_1$ dimer, as assessed by two-electrode voltage clamp analysis (Fig. 6A). Likewise, SDS-PAGE analysis of the surface radioiodinated P2X$_1$ dimer-derived polypeptides and subsequent quantification by PhosphorImaging of the monomer-to-dimer ratio at the plasma membrane showed no significant reduction of monomer formation upon deletion of internal methionines or the hexahistidyl tag (Fig. 6, B and C). Taken together these results argue against an important role of internal translation initiation in the generation of monomers from cRNA encoding concatenated P2X$_1$ dimers.

The Monomeric Byproduct Originates Predominantly from the P2X$_1$ Copy in the N-Terminal Position. Alternative mechanisms that may lead to the generation of monomeric byproducts are premature termination of translation and proteolytic cleavage of full-length concatamers. Whereas premature translation termination can be expected to favor the expression of the leading copy of a concatenated P2X$_1$ dimer, proteolytic cleavage within the linker region may produce two functional P2X$_1$ monomers. To discriminate between these possibilities, we examined whether or not both copies of a P2X$_1$ dimer contribute equally to the generation of monomeric byproducts. To this end, we took advantage of a nonfunctional His-P2X$_1^{R34L}$ mutant, which is exported to the plasma membrane as a noncovalently linked trimer but does not mediate any ATP-gated inward current (results not shown). Concatenated P2X$_1$ dimers were tagged with this nonfunctional His-P2X$_1^{R34L}$ subunit either at the N-terminal or the C-terminal position. Recording of the ATP-gated currents in oocytes expressing the concatenated dimer constructs showed significantly larger currents when the nonfunctional His-P2X$_1^{R34L}$ subunit was at the C-terminal rather than at the N-terminal position. The relatively low current amplitudes observed from tandem dimers containing

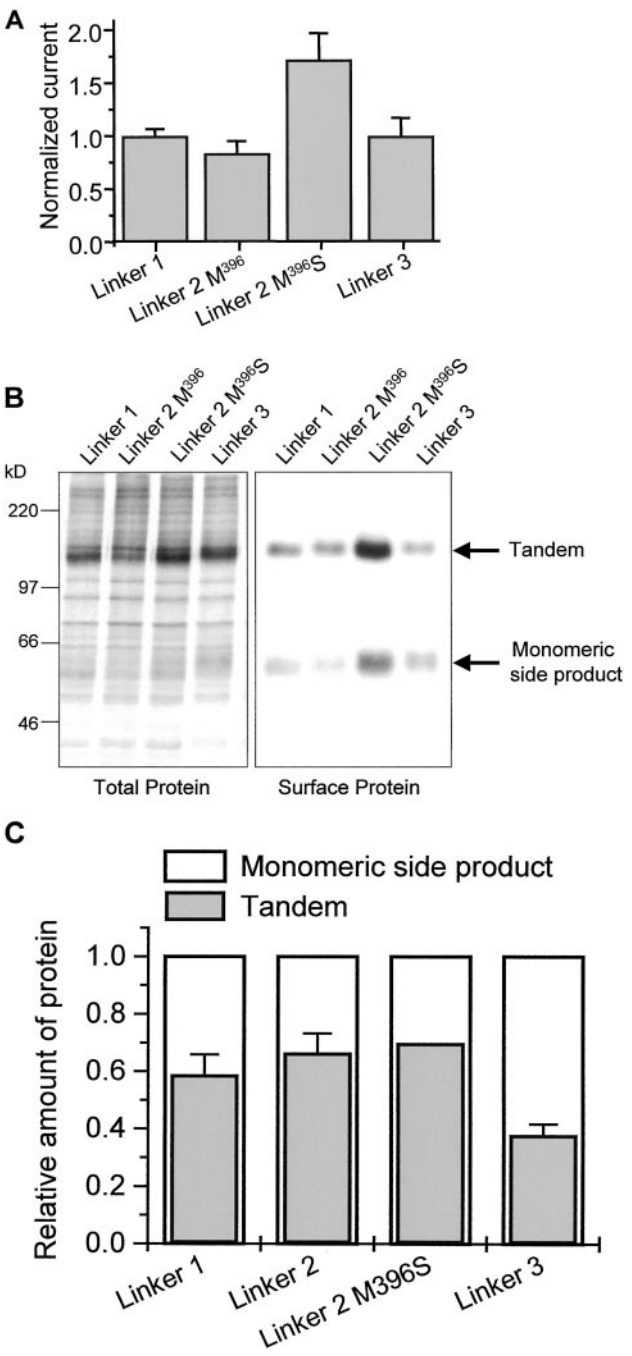

Fig. 6. Effect of linker sequence on formation of monomeric side product from expressed tandem His-P2X$_1$ dimers. Subgroups of oocytes injected with the indicated cRNAs were either labeled with [^{35}S]methionine or kept unlabeled for later electrophysiological analysis and surface radioiodination. All oocytes were analyzed in parallel 3 days after cRNA injection. A, magnitudes of inward currents elicited by 30 μM ATP were recorded at -60 mV. Data are given as means $\pm$ S.E.M. from 22 to 36 oocytes per column analyzed in two to five independent experiments. B, subgroups of the same oocytes were either metabolically labeled overnight and then chased for 2 days or radioiodinated with ^{125}I-sulfo-SHPP at day 3 after cRNA injection. His-tagged proteins were isolated from dodecylmaltoside extracts (0.5%) of the oocytes and resolved by reducing SDS-PAGE (8% acrylamide). C, shown are the amounts of concatenated dimers normalized to the respective monomeric byproduct, as determined by PhosphorImaging. Data are means $\pm$ S.E.M. from three independent experiments except for the tandem dimer with linker 2 and the M^{396}S mutation, which was analyzed in a single experiment only (with identical results in duplicate determinations). Note that the monomeric side product was always present in larger amounts than the tandem dimers, suggesting that dimers require to combine with a monomer for export to the cell surface.

one copy of the $R^{34}L$ mutant compared with the His-$P2X_1$ dimer suggests a dominant-negative effect of the $R^{34}L$ mutation, which may lead to a nonfunctional receptor even if only one copy of this mutant is incorporated into a trimeric channel complex.

Discussion

In the present study, we exploited the concatamer approach for the determination of the subunit stoichiometry of the homomeric $P2X_1$ receptor. We show that $P2X_1$ concatamers up to the hexamer are readily synthesized in *X. laevis* oocytes as full-length glycoproteins, yet the plasma membrane contains monomeric and dimeric byproducts of the $P2X_1$ concatamers rather than the full-length concatamers. These byproducts exist as complexes of one dimer plus one monomer or three monomers (Fig. 7) and are thus indistinguishable in mass from an authentic homotrimeric $P2X_1$ receptor formed upon expression of nonconcatenated $P2X_1$ subunits. We infer from these results that ATP-gated inward currents that could be elicited from all oocytes irrespective of the order of the concatamer expressed are largely mediated by receptor complexes assembled from monomeric and dimeric byproducts, which accordingly constitute the principal functional elements of higher order $P2X_1$ concatamers. The sole full-length concatamers that appear in significant amounts at the plasma membrane are the $P2X_1$ dimer and trimer, but in these cases, similar or even higher amounts of the monomeric byproduct are also present.

Possible Origin of Lower Order Byproducts. Any explanation of the origin of the lower order byproducts has to take into account that (i) only uniform populations of both monomers and dimers are produced, which have exactly the length of one copy or two copies of a $P2X_1$ polypeptide, respectively, and that (ii) functional $P2X_1$ receptors include predominantly the leading $P2X_1$ copy of tandem dimers. These observations exclude partially degraded cRNA, unspecific proteolytic degradation, and internal translation initiation within the linker region as a possible source of byproducts. The latter was further ruled out by mutational deletion of ATGs shortly before and within the linker sequence, which did not reduce the formation of monomers from tandem dimers. Premature termination of translation because of unfavorable secondary cRNA structures in the linker region could basically explain both the truncation after the first or second repeat and the prominent role of the leading $P2X_1$ copy of tandem dimers to the formation of functional receptors. However, computational analysis provided no indication for the presence of stable hairpin-like structures. Even more importantly, no lower order byproducts were seen upon translation of the concatamers in vitro (results not shown), indicating that byproduct formation requires intact cells.

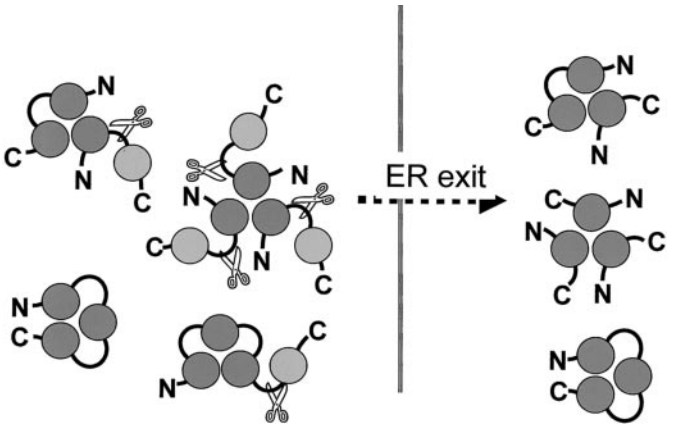

Fig. 7. Cartoon showing the formation of trimeric $P2X_1$ receptors from concatenated $P2X_1$ dimers, trimers, and tetramers. The left hand displays possible subunit arrangements of concatamers comprising two to four $P2X_1$ subunit copies in the ER. Inconsistencies with the concatamer approach have previously been attributed to the exclusion of individual copies (▨) of a given concatamer from a functional arrangement of subunits around an ion pore. In the case of $P2X_1$ concatamers, however, only concatenated $P2X_1$ trimers appear at the plasma membrane by themselves (right). Dimers can only exit the ER after combining noncovalently with a $P2X_1$ monomer, formed as a byproduct and representing the leading copy of another $P2X_1$ dimer. Alternatively, three such monomeric byproducts corresponding to the leading copies of three dimers can noncovalently assemble to a trimeric $P2X_1$ receptor complex. Finally, the fourth copy of a concatenated tetramer can be cleaved off to yield a concatenated $P2X_1$ trimer that can exit the ER. Altogether, although full-length $P2X_1$ concatamers are efficiently synthesized in *X. laevis* oocytes, solely proteins equivalent to three $P2X_1$ subunit copies are exported to the plasma membrane.

Impaired transmembrane folding of the second copy of a tandem dimer, such that only the leading copy acquires a native conformation, could also account for the prominent role of the leading $P2X_1$ copy and even explain the strong propensity of full-length concatamers to aggregate. It is possible that the membrane integration of the numerous transmembrane segments of higher order concatamers is difficult to achieve. By serving as alternate signal anchor and stop transfer sequences, two transmembrane segments may suffice to assure the correct transmembrane disposition of a $P2X_1$ monomer. However, additional internal topogenic motifs might be required to assure the correct sequential insertion of four and more transmembrane segments with altering orientations. The carbohydrate content is indicative of the usage of all *N*-glycosylation sites, suggesting that proper transmembrane folding occurs. On the other hand, a concatamer that acquires only the most proximal three (or five) transmembrane segments would also become fully glycosylated if the entire polypeptide chain behind the third (or fifth) transmembrane domain is targeted into the ER lumen, where it would constitute an unusable appendage. This could lead to exposure of hydrophobic surfaces that could interact to form aggregates. If the misfolded portion of the concatamer were a substrate for proteases, selective degradation of the misfolded portion of a concatamer would leave a correctly folded monomer.

It should be emphasized that the lower order byproducts represent only a negligible fraction of the total population of $P2X_1$ polypeptides synthesized, indicating that the byproducts are generated by a rather inefficient mechanism. It is even possible that the generation of the byproducts is the direct consequence of an accumulation of improperly folded concatamers in the ER. Currents that arise from proteins assembled solely from minute amounts of byproducts can nevertheless be recorded easily because of the sensitivity of electrophysiological techniques.

Concatamer Strategy. Although the usefulness of the concatamer approach has been carefully documented (see *Introduction*), several electrophysiological studies suggest that the tandem linkage does not always ensure the subunit stoichiometry (McCormack et al., 1992; Liman et al., 1992; Hurst et al., 1995). Even in studies with otherwise well

constrained stoichiometry, certain concatenated K_v trimers and pentamers (Liman et al., 1992), as well as certain K_{ir} trimers (Silverman et al., 1996), unexpectedly yielded large currents when expressed alone. Such inconsistencies with the concatamer approach have generally been attributed to the multimerization of full-length concatamers (McCormack et al., 1992; Hurst et al., 1995; Yang et al., 1995; Shapiro and Zagotta, 1998; Stoop et al., 1999). In this way, one or several repeats of separate concatamers become incorporated into a channel, leaving other repeats of the same polypeptides outside the channel.

In the few studies, in which biochemical data have also been provided, the synthesis of full-length concatamers was demonstrated by in vitro translation in rabbit reticulocyte lysate (Tu and Deutsch, 1999) or immunoblotting of oocyte-expressed protein (Tytgat et al., 1996; Firsov et al., 1998; Newbolt et al., 1998; Köhler et al., 2000). Biochemical studies on oligomerization of concatamers were done on yeast or *E. coli* expressed proteins (Mathai and Agre, 1999; Sukharev et al., 1999). However, no differentiation between plasma membrane-bound protein, which is amenable to functional analysis, and total protein was made. In our experiments, the detection of the small amounts of lower order byproducts and their parent $P2X_1$ receptor-like assembly behavior depended critically on the visualization of plasma membrane-bound polypeptides and their oligomeric state by surface radioiodination and blue native PAGE analysis, respectively. Hence, it is very possible that small amounts of lower order byproducts remained undetected in some of the previous investigations and that the formation of lower order side products rather than oligomerization of concatamers is responsible for the inconsistencies observed in previous studies.

Trimeric Architecture of P2X Receptors. The present data demonstrate that the concatamer approach does not assure the subunit arrangement of the $P2X_1$ receptor but nonetheless corroborates the trimeric structure of $P2X_1$ receptors. First, the concatenated $P2X_1$ trimer migrates exactly with the same mobility as the parent $P2X_1$ receptor consisting of three noncovalently linked monomers. Second, monomers and dimers appear at the plasma membrane in approximately stoichiometric amounts, suggesting that the amount of monomers available to combine with dimers most likely constitutes the limiting factor for ER exit of full-length $P2X_1$ dimers to the plasma membrane; hence, a trimer constitutes the sole complex that can adopt a conformation able to pass the quality control system. Third, tetramers are not exported to the plasma membrane, indicating that tetramers can adopt only a non-native conformation that does not allow for ER exit. Fourth, free dimers (i.e., those without an associated monomer) or oligomerized dimers such as tetramers or hexamers were not observed to occur at the plasma membrane. In our previous study, we could not exclude that $P2X_1$ trimers assemble to form larger entities such as hexamers and nonamers. From the present observation, we infer that trimers constitute the sole $P2X_1$ receptor conformation capable of passing the ER quality control system; hence, trimers represent the "correct" architecture of homomeric $P2X_1$ receptors.

A trimeric structure of P2X receptors was also deduced from an electrophysiological analysis of concatenated $P2X_2$ subunits (Stoop et al., 1999), which relied on the extent of current inhibition by a cysteine-reactive compound (methanethiosulfonate ethyltrimethylammonium) of $P2X_2$ concatamers of different lengths composed of wild-type and mutant $P2X_2$ subunits. Notably, also in this study, a preference for incorporation of the N terminal subunits was observed. Moreover, currents could be evoked by ATP in all oocytes expressing concatamers up to a $P2X_2$ hexamer, which may indicate that lower order byproducts contributed to the formation of functional $P2X_2$ receptors. In contrast to our study, significantly higher current amplitudes were determined in oocytes expressing the trimeric $P2X_2$ construct rather than dimers, tetramers, or hexamers. This may signify that the fraction of full-length concatamers that appeared at the plasma membrane compared with those that were retained in the ER is more favorable with $P2X_2$ concatamers than with $P2X_1$ concatamers.

A major obstacle with concatenated $P2X_1$ subunits seems to be their limited capacity to adopt a properly folded conformation, as evidenced by their propensity to form large aggregates, which cannot exit the ER. This observation raises the question of whether a homotrimer of concatenated $P2X_1$ subunits really corresponds to the subunit order of native $P2X_1$ receptors. The poor expression of homomeric $P2X_1$ concatamers could result from the lack of a "β subunit", which, if concatenated in the correct neighborhood relationship to $P2X_1$ subunits, would guide efficient assembly. Candidate subunits are $P2X_2$ and $P2X_5$ subunits, which have both been observed to heteropolymerize with $P2X_1$ subunits (Lê et al., 1999; Brown et al., 2002). Hence, our data might argue against the existence of homomeric $P2X_1$ receptors as naturally occurring receptors. It must be noted, however, that P2X receptors are efficiently formed in a variety of heterologous expression systems. This is in marked contrast to a variety of other receptor subunits, including $P2X_6$ subunits and several members of the nicotinic superfamily, which seem to operate exclusively as heteromultimers and express very poorly or not at all from incomplete subunit combinations. Expression of incomplete subunit combinations of the muscle-type nAChR, for instance, resulted in the formation of a significant amount of aggregated subunits (Nicke et al., 1999). Moreover, our labeling experiments provided no evidence for the assembly of $P2X_1$ subunits with polypeptides originating from *X. laevis* oocytes, yet showed that complete homotrimerization was accomplished during or shortly after synthesis; free monomers and dimers or aggregated $P2X_1$ subunits were never observed.

Taken together, we conclude that the inefficient formation of functional ion channels from $P2X_1$ concatamers does not argue against the existence of homotrimeric $P2X_1$ receptors; rather, it results from subunit concatenation for reasons that are unclear at present. Artificially concatenated K^+ channel subunits have natural counterparts, such as tandem of P domains in a weak inwardly rectifying K^+ channel (TwiK), which contain the equivalent of two K_{ir} subunits in tandem in one polypeptide or 2 P region containing outwardly rectifying K^+ channel (ToK), which corresponds to a K_v channel subunit tethered with a K_{ir} subunit. In addition, K^+ channels belong to a protein superfamily that includes Na^+ and Ca^{2+} channels, which can be regarded as naturally occurring concatamers formed by single large polypeptides with four internally homologous repeats. These overall similarities may explain why the concatamer approach works particularly well with K^+ channel subunits and such congeners as cyclic nucleotide-gated channels. On the other hand, as discussed

above, inconsistencies have been noted even in studies with concatenated K^+ channel subunits. In particular, a preferred incorporation of the leading subunits into the channel complex was reported in several studies (Liman et al., 1992; McCormack et al., 1992; Shapiro and Zagotta, 1998; Stoop et al., 1999), suggesting that lower order byproducts are not unique to $P2X_1$ concatamers but can occur with concatamers of other proteins as well. Biochemical visualization of the plasma membrane-bound ion channel might therefore be of crucial importance to avoid misinterpretation of electrophysiological data from concatenated polypeptides.

References

Baumann SW, Baur R, and Sigel E (2001) Subunit arrangement of γ-aminobutyric acid type A receptors. *J Biol Chem* **276:**36275–36280.

Blount P, Sukharev SI, Moe PC, Schroeder MJ, Guy HR, and Kung C (1996) Membrane topology and multimeric structure of a mechanosensitive channel protein of *Escherichia coli*. *EMBO (Eur Mol Biol Organ) J* **15:**4798–4805.

Brown SG, Townsend-Nicholson A, Jacobson KA, Burnstock G, and King BF (2002) Heteromultimeric $P2X_{1/2}$ receptors show a novel sensitivity to extracellular pH. *J Pharmacol Exp Ther* **300:**673–680.

Emerick MC and Fambrough DM (1993) Intramolecular fusion of Na pump subunits assures exclusive assembly of the fused α subunit and β subunit domains into a functional enzyme in cells also expressing endogenous Na pump subunits. *J Biol Chem* **268:**23455–23459.

Firsov D, Gautschi I, Merillat AM, Rossier BC, and Schild L (1998) The heterotetrameric architecture of the epithelial sodium channel (ENaC). *EMBO (Eur Mol Biol Organ) J* **17:**344–352.

Griffon N, Büttner C, Nicke A, Kuhse J, Schmalzing G, and Betz H (1999) Molecular determinants of glycine receptor subunit assembly. *EMBO (Eur Mol Biol Organ) J* **18:**4711–4721.

Heginbotham L and Mackinnon R (1992) The aromatic binding site for tetraethylammonium ion on potassium channels. *Neuron* **8:**483–491.

Hurst RS, Kavanaugh MP, Yakel J, Adelman JP, and North RA (1992) Cooperative interactions among subunits of a voltage-dependent potassium channel. Evidence from expression of concatenated cDNAs. *J Biol Chem* **267:**23742–23745.

Hurst RS, North RA, and Adelman JP (1995) Potassium channel assembly from concatenated subunits: effects of proline substitutions in S4 segments. *Recept Channels* **3:**263–272.

Im WB, Pregenzer JF, Binder JA, Dillon GH, and Alberts GL (1995) Chloride channel expression with the tandem construct of α6-β2 $GABA_A$ receptor subunit requires a monomeric subunit of α6 or γ2. *J Biol Chem* **270:**26063–26066.

Isacoff EY, Jan YN, and Jan LY (1990) Evidence for the formation of heteromultimeric potassium channels in *Xenopus* oocytes. *Nature (Lond)* **345:**530–534.

Kavanaugh MP, Hurst RS, Yakel J, Varnum MD, Adelman JP, and North RA (1992) Multiple subunits of a voltage-dependent potassium channel contribute to the binding site for tetraethylammonium. *Neuron* **8:**493–497.

Kirsch GE, Pascual JM, and Shieh CC (1995) Functional role of a conserved aspartate in the external mouth of voltage-gated potassium channels. *Biophys J* **68:**1804–1813.

Köhler K, Forster IC, Lambert G, Biber J, and Murer H (2000) The functional unit of the renal type IIa Na^+/P_i cotransporter is a monomer. *J Biol Chem* **275:**26113–26120.

Lee TE, Philipson LH, Kuznetsov A, and Nelson DJ (1994) Structural determinant for assembly of mammalian K^+ channels. *Biophys J* **66:**667–673.

Lee TE, Philipson LH, and Nelson DJ (1996) N-Type inactivation in the mammalian *Shaker* K^+ channel Kv1.4. *J Membr Biol* **151:**225–235.

Lê KT, Boue-Grabot E, Archambault V, and Séguela P (1999) Functional and biochemical evidence for heteromeric ATP-gated channels composed of $P2X_1$ and $P2X_5$ subunits. *J Biol Chem* **274:**15415–15419.

Liman ER, Tytgat J, and Hess P (1992) Subunit stoichiometry of a mammalian K^+ channel determined by construction of multimeric cDNAs. *Neuron* **9:**861–871.

Liu DT, Tibbs GR, and Siegelbaum SA (1996) Subunit stoichiometry of cyclic nucleotide-gated channels and effects of subunit order on channel function. *Neuron* **16:**983–990.

Mackenzie AB, Surprenant A, and North RA (1999) Functional and molecular diversity of purinergic ion channel receptors. *Ann NY Acad Sci* **868:**716–729.

Mathai JC and Agre P (1999) Hourglass pore-forming domains restrict aquaporin-1 tetramer assembly. *Biochemistry* **38:**923–928.

McCormack K, Lin L, Iverson LE, Tanouye MA, and Sigworth FJ (1992) Tandem linkage of *Shaker* K^+ channel subunits does not ensure the stoichiometry of expressed channels. *Biophys J* **63:**1406–1411.

Newbolt A, Stoop R, Virginio C, Surprenant A, North RA, Buell G, and Rassendren F (1998) Membrane topology of an ATP-gated ion channel (P2X Receptor). *J Biol Chem* **273:**15177–15182.

Nicke A, Bäumert HG, Rettinger J, Eichele A, Lambrecht G, Mutschler E, and Schmalzing G (1998) $P2X_1$ and $P2X_3$ receptors form stable trimers: a novel structural motif of ligand-gated ion channels. *EMBO (Eur Mol Biol Organ) J* **17:**3016–3028.

Nicke A, Rettinger J, Mutschler E, and Schmalzing G (1999) Blue native PAGE as a useful method for the analysis of the assembly of distinct combinations of nicotinic acetylcholine receptor subunits. *J Recept Signal Transduct Res* **19:**493–507.

Pessia M, Tucker SJ, Lee K, Bond CT, and Adelman JP (1996) Subunit positional effects revealed by novel heteromeric inwardly rectifying K^+ channels. *EMBO (Eur Mol Biol Organ) J* **15:**2980–2987.

Rettinger J, Aschrafi A, and Schmalzing G (2000) Roles of individual *N*-glycans for ATP potency and expression of the rat $P2X_1$ receptor. *J Biol Chem* **275:**33542–33547.

Sahin-Tóth M, Lawrence MC, and Kaback HR (1994) Properties of permease dimer, a fusion protein containing two lactose permease molecules from *Escherichia coli*. *Proc Natl Acad Sci USA* **91:**5421–5425.

Schägger H, Cramer WA, and von Jagow G (1994) Analysis of molecular masses and oligomeric states of protein complexes by blue native electrophoresis and isolation of membrane protein complexes by two-dimensional native electrophoresis. *Anal Biochem* **217:**220–230.

Shapiro MS and Zagotta WN (1998) Stoichiometry and arrangement of heteromeric olfactory cyclic nucleotide-gated ion channels. *Proc Natl Acad Sci USA* **95:**14546–14551.

Silverman SK, Lester HA, and Dougherty DA (1996) Subunit stoichiometry of a heteromultimeric G protein-coupled inward-rectifier K^+ channel. *J Biol Chem* **271:**30524–30528.

Stoop R, Thomas S, Rassendren F, Kawashima E, Buell G, Surprenant A, and North RA (1999) Contribution of individual subunits to the multimeric $P2X_2$ receptor: estimates based on methanethiosulfonate block at T336C. *Mol Pharmacol* **56:**973–981.

Sukharev SI, Schroeder MJ, and McCaslin DR (1999) Stoichiometry of the large conductance bacterial mechanosensitive channel of E. coli. A biochemical study. *J Membr Biol* **171:**183–193.

Torres GE, Egan TM, and Voigt MM (1998) Topological analysis of the ATP-gated ionotrophic $P2X_2$ receptor subunit. *FEBS Lett* **425:**19–23.

Tu L and Deutsch C (1999) Evidence for dimerization of dimers in K^+ channel assembly. *Biophys J* **76:**2004–2017.

Tytgat J, Buyse G, Eggermont J, Droogmans G, Nilius B, and Daenens P (1996) Do voltage-gated Kv1.1 and inward rectifier Kir2.1 potassium channels form heteromultimers? *FEBS Lett* **390:**280–284.

Tytgat J, Nakazawa K, Gross A, and Hess P (1993) Pursuing the voltage sensor of a voltage-gated mammalian potassium channel. *J Biol Chem* **268:**23777–23779.

Ulens C and Tytgat J (2001) Functional heteromerization of HCN1 and HCN2 pacemaker channels. *J Biol Chem* **276:**6069–6072.

Varnum MD and Zagotta WN (1996) Subunit interactions in the activation of cyclic nucleotide-gated ion channels. *Biophys J* **70:**2667–2679.

Yang J, Jan YN, and Jan LY (1995) Determination of the subunit stoichiometry of an inwardly rectifying potassium channel. *Neuron* **15:**1441–1447.

Address correspondence to: Günther Schmalzing, M.D. Department of Molecular Pharmacology, Wendlingweg 2, D-52074 Aachen, Germany. E-mail gschmalzing@ukaachen.de